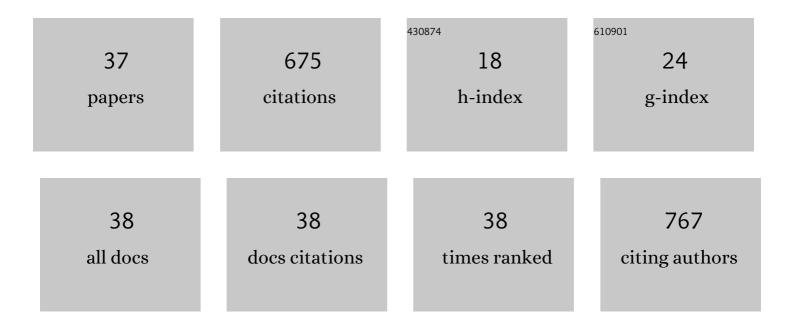
Sanjit Dey

List of Publications by Year in descending order

Source: https://exaly.com/author-pdf/7606689/publications.pdf Version: 2024-02-01



SANUT DEV

#	Article	IF	CITATIONS
1	A napthelene–pyrazol conjugate: Al(<scp>iii</scp>) ion-selective blue shifting chemosensor applicable as biomarker in aqueous solution. Analyst, The, 2014, 139, 4828-4835.	3.5	44
2	A detailed theoretical DFT study of the hydrolysis mechanism of orally active anticancer drug ZD0473. Chemical Physics Letters, 2010, 487, 108-115.	2.6	30
3	Fluorescent Guar Gum- <i>g</i> -Terpolymer via In Situ Acrylamido-Acid Fluorophore-Monomer in Cell Imaging, Pb(II) Sensor, and Security Ink. ACS Applied Bio Materials, 2020, 3, 1995-2006.	4.6	30
4	Role of non-covalent interactions in the supramolecular architectures of mercury(<scp>ii</scp>) diphenyldithiophosphates: An experimental and theoretical investigation. New Journal of Chemistry, 2021, 45, 2249-2263.	2.8	29
5	Radiosensitizing effect of ellagic acid on growth of Hepatocellular carcinoma cells: an in vitro study. Scientific Reports, 2017, 7, 14043.	3.3	28
6	Fluorescent Terpolymers via In Situ Allocation of Aliphatic Fluorophore Monomers: Fe(III) Sensor, Highâ€Performance Removals, and Bioimaging. Advanced Healthcare Materials, 2019, 8, 1900980.	7.6	28
7	An insight into the non-covalent Pb⋯S and S⋯S interactions in the solid-state structure of a hemidirected lead(<scp>ii</scp>) complex. CrystEngComm, 2020, 22, 237-247.	2.6	28
8	Synthesis of Biocompatible Aliphatic Terpolymers via In Situ Fluorescent Monomers for Three-in-One Applications: Polymerization of Hydrophobic Monomers in Water. Langmuir, 2020, 36, 6178-6187.	3.5	28
9	Fluorescent Terpolymers Using Two Non-Emissive Monomers for Cr(III) Sensors, Removal, and Bio-Imaging. ACS Biomaterials Science and Engineering, 2020, 6, 1397-1407.	5.2	26
10	Phenoxo-bridged dinuclear mixed valence cobalt(<scp>iii</scp> / <scp>ii</scp>) complexes with reduced Schiff base ligands: synthesis, characterization, band gap measurements and fabrication of Schottky barrier diodes. Dalton Transactions, 2021, 50, 1721-1732.	3.3	25
11	Magnetic Properties of End-to-End Azide-Bridged Tetranuclear Mixed-Valence Cobalt(III)/Cobalt(II) Complexes with Reduced Schiff Base Blocking Ligands and DFT Study. ACS Omega, 2019, 4, 20634-20643.	3.5	23
12	Synthesis, characterization, self-assembly and non-ohmic Schottky barrier diode behaviors of two iron(<scp>iii</scp>) based semiconductors with theoretical insight. CrystEngComm, 2020, 22, 5170-5181.	2.6	23
13	Multiâ€Câ^'C/Câ^'Nâ€Coupled Lightâ€Emitting Aliphatic Terpolymers: Nâ^'Hâ€Functionalized Fluorophore Monomers and Highâ€Performance Applications. Chemistry - A European Journal, 2020, 26, 502-516.	3.3	21
14	DFT study on the redox behavior of two dioxovanadium(<scp>v</scp>) complexes with N ₂ O donor Schiff base ligands and their use in catalytic oxidation of <i>ortho</i> -aminophenol. New Journal of Chemistry, 2019, 43, 18747-18759.	2.8	20
15	Light-Emitting Multifunctional Maleic Acid- <i>co</i> -2-(<i>N</i> -(hydroxymethyl)acrylamido)succinic Acid- <i>co</i> - <i>N</i> -(hydroxymethyl)acrylamide for Fe(III) Sensing, Removal, and Cell Imaging. ACS Omega, 2020, 5, 3333-3345.	3.5	20
16	Cyclometalated rhodium(III) complexes bearing dithiocarbamate derivative: Synthesis, characterization, interaction with DNA and biological study. Polyhedron, 2014, 69, 127-134.	2.2	19
17	Substituent effect on fluorescence signaling of the cell permeable HSO ₄ ^{â^'} receptors through single point to ratiometric response in green solvent. RSC Advances, 2014, 4, 27665-27673.	3.6	19
18	Quantum chemical predictions of aqueous pK values for OH groups of some α-hydroxycarboxylic acids based on ab initio and DFT calculations. Computational and Theoretical Chemistry, 2018, 1125, 29-38.	2.5	19

SANJIT DEY

#	Article	IF	CITATIONS
19	A theoretical insight on the rigid hydrogen-bonded network in the solid state structure of two zinc(<scp>ii</scp>) complexes and their strong fluorescence behaviors. CrystEngComm, 2020, 22, 3005-3019.	2.6	19
20	Synthesis, characterization, interactions with DNA and bovine serum albumin (BSA), and antibacterial activity of cyclometalated iridium(III) complexes containing dithiocarbamate derivatives. Journal of Coordination Chemistry, 2014, 67, 2643-2660.	2.2	18
21	Field-induced single molecule magnet behavior of a dinuclear cobalt(<scp>ii</scp>) complex: a combined experimental and theoretical study. Dalton Transactions, 2020, 49, 16778-16790.	3.3	18
22	A mixed phenoxo and end-on azide bridged dinuclear copper(<scp>ii</scp>) Schiff base complex: synthesis, structure, magnetic characterization and DFT study. New Journal of Chemistry, 2018, 42, 13512-13519.	2.8	16
23	Understanding the Difference in Photophysical Properties of Cyclometalated Iridium(III) and Rhodium(III) Complexes by Detailed Time-Dependent Density Functional Theory and Frontier Molecular Orbital Supports. Journal of Physical Chemistry C, 2017, 121, 11632-11642.	3.1	15
24	Relative stability of the <i>cis</i> and <i>trans</i> isomers of octahedral cobalt(<scp>iii</scp>) complexes of the type [Co(N ₂ O ₂)X ₂] with tetradentate salen type Schiff bases: a combined theoretical and experimental study. CrystEngComm, 2019, 21, 6026-6037.	2.6	15
25	Understanding a Thermoemissive ESIPT-Based Solid-State Off–On Switch as a Dual-Channel Chemosensor in Solid and Solution Phases: Detailed Experimental and Theoretical Study. Journal of Physical Chemistry C, 2020, 124, 18181-18193.	3.1	15
26	A detailed quantum chemical study of the interactions of [Pt(dien)Cl]+ with a series of S-donor ligands: A computational approach. Computational and Theoretical Chemistry, 2012, 991, 116-123.	2.5	14
27	Synthesis, structure, DFT study and catechol oxidase activity of Cu(II) complex with sterically constrained phenol based ligand. Journal of Molecular Structure, 2019, 1193, 265-273.	3.6	14
28	trans-Platinum anticancer drug AMD443: A detailed theoretical study by DFT–TST method on the hydrolysis mechanism. Chemical Physics Letters, 2010, 497, 142-148.	2.6	13
29	A detailed theoretical study of the interaction of thiourea with cis-diaqua(ethylenediamine) platinum(II). Computational and Theoretical Chemistry, 2009, 913, 97-106.	1.5	12
30	An insight into the interaction between α-ketoamide- based inhibitor and coronavirus main protease: A detailed in silico study. Biophysical Chemistry, 2021, 269, 106510.	2.8	11
31	An oxorhenium(V) Schiff-base complex: synthesis, structure, spectroscopic characterization, electrochemistry, and DFT calculations. Journal of Coordination Chemistry, 2013, 66, 1178-1188.	2.2	10
32	Understanding the ring-opening, chelation and non-chelation reactions between nedaplatin and thiosulfate: a DFT study based on NBO, ETS-NOCV and QTAIM. Theoretical Chemistry Accounts, 2016, 135, 1.	1.4	5
33	Effect of Main Versus Ancillary Ligand Substitution on the Photophysical Properties of a Series of Ir(III) Complexes: A Detailed Theoretical Investigation. Journal of Physical Chemistry A, 2020, 124, 4654-4665.	2.5	5
34	Synthesis, characterization and self assembly of dinuclear zinc Schiff base complexes: A combined experimental and theoretical study. Polyhedron, 2022, 225, 116044.	2.2	5
35	Interactions of the aquated forms of the anticancer drug AMD443 with DNA purine bases: A detailed computational approach. Inorganica Chimica Acta, 2013, 400, 130-141.	2.4	4
36	Efficient and Convenient Methods for Synthesis of Some Phthalazine Derivatives and Their Evaluation of Cytotoxicity. Synthetic Communications, 2014, 44, 847-857.	2.1	3

#	Article	IF	CITATIONS
37	A mononuclear zinc complex with a diamine: Synthesis, characterization, self assembly, luminescence property and DFT calculations. Journal of Molecular Structure, 2022, 1249, 131598.	3.6	3